Liquid Crystals
Publication details, including instructions for authors and subscription information:
http://www.informaworld.com/smpp/title~content=t713926090

Alignment and switching of AFLC materials using various boundary conditions

Artur Adamski[a]; Kristiaan Neyts[a]; Koen D'havé[b]; Per Rudquist[b]; Roman Dąbrowski[c]
[a] Ghent University, Electronics and Information Systems Department, LCD Research Group, B-9000 Gent, Belgium [b] Chalmers University of Technology, Department of Microtechnology and Nanoscience, Photonics Laboratory, Liquid Crystal Group, 41296 Göteborg, Sweden [c] Military University of Technology, Institute of Chemistry, 00-908 Warszawa, Poland

To cite this Article Adamski, Artur , Neyts, Kristiaan , D'havé, Koen , Rudquist, Per and Dąbrowski, Roman(2005) 'Alignment and switching of AFLC materials using various boundary conditions', Liquid Crystals, 32: 6, 707 — 715
To link to this Article: DOI: 10.1080/02678290500117621
URL: http://dx.doi.org/10.1080/02678290500117621

Liquid Crystals, Vol. 32, No. 6, June 2005, 707–715

Taylor & Francis
Taylor & Francis Group

Alignment and switching of AFLC materials using various boundary conditions

ARTUR ADAMSKI*†, KRISTIAAN NEYTS†, KOEN D'HAVÉ‡, PER RUDQUIST‡ and ROMAN DĄBROWSKI§

†Ghent University, Electronics and Information Systems Department., LCD Research Group, St.Pietersnieuwstraat 41, B-9000 Gent, Belgium

‡Chalmers University of Technology, Department of Microtechnology and Nanoscience, Photonics Laboratory, Liquid Crystal Group, Kemivägen 9, 41296 Göteborg, Sweden

§Military University of Technology, Institute of Chemistry, ul. Kaliskiego 2, 00-908 Warszawa, Poland

(*Received 17 January 2005; accepted 10 February 2005*)

We have systematically studied the quality of bookshelf alignment and electro-optic characteristics of two antiferroelectric liquid crystal materials in cells with various boundary conditions. The electro-optic characteristics of the materials studied depend strongly on both the liquid crystal materials and the boundary conditions at the supporting substrates. We have compared a number of observations in these cells: the tendency to form AFLC domains in the virgin state and after switching; the surface electroclinic effect (SEC effect); the transmission–voltage characteristics (TV) when driven with triangular- and square-wave voltages at various frequencies; the threshold field and the conditions for relaxation to the AFLC state. The set of samples includes specially designed and manufactured test cells with different polyimides as alignment layers, treated with varying rubbing strengths. We discuss the significance of various factors and show the importance of simultaneously optimizing both materials and cell parameters for AFLC applications.

1. Introduction

In liquid crystal (LC) electro-optic devices, e.g. information displays, the LC orientation in the absence of external electric fields is given by the boundary conditions. These are in turn defined by the surface alignment layers and their treatment. Typically, the alignment layers consist of thin (~100 nm) polymer films deposited on the inner cell surfaces and subsequently mechanically and unidirectionally rubbed with a cloth. The LC molecules close to the surfaces tend to align along the rubbing direction and this orientation is transferred to the bulk through elastic forces [1]. Unfortunately the mechanisms that govern the alignment are still not well understood. In a nematic LC, where only orientational order is present, the molecules tend to align rather easily along the rubbing direction. In smectics, like ferroelectric and antiferroelectric (SmC* and SmC_a*) LCs, where one-dimensional positional order is also present, the alignment mechanisms become much more complex. Smectic materials are used in the 'bookshelf structure', see figure 1. This structure is formed in planar orienting cells at the transition from the nematic to SmA* phase. Through the phase transition the director (**n**) orientation of the nematic phase is maintained and the smectic layers of the SmA are formed perpendicular to the buffing direction. In the absence of a nematic phase between the isotropic and the smectic phases—as in antiferroelectric liquid crystals and V-shaped switching ferroelectric materials—there is a well known problem in obtaining a homogeneous bookshelf structure. Moreover, the so-called surface electroclinic effect [2] allowed by the chirality, makes the smectic layer normal **k** deviate a certain angle away from the rubbing direction in these materials. In addition to this, chevron configurations due to the

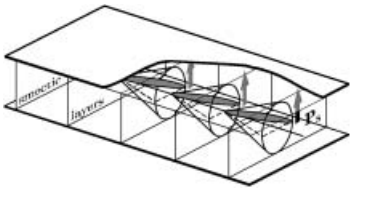

Figure 1. Bookshelf structure of smectic materials. Molecules are grouped in homogeneous layers, which are perpendicular to the constraining surfaces.

*Corresponding author. Email: adamsart@elis.ugent.be

Liquid Crystals
ISSN 0267-8292 print/ISSN 1366-5855 online © 2005 Taylor & Francis Group Ltd
http://www.tandf.co.uk/journals
DOI: 10.1080/02678290500117621

smectic layer shrinkage when cooling from the SmA* to SmC* (resulting in zig-zag defects) [3], layer straightening effects (horizontal chevrons) [4] and striped textures [5] also destroy the alignment uniformity and degrade the electro-optic characteristics of the device. Basic parameters such as static and dynamic light leakage (often referred to as a pretransitional effect), brightness, contrast ratio and threshold voltage all critically depend on the nature and quality of alignment.

In this paper we explicitly show how different surface alignment layers and rubbing conditions may affect both the quality of the bookshelf structure and the electro-optic performance of three high tilt AFLC mixtures. We also show the importance of choosing a proper *combination* of a specific AFLC material, alignment layer, and rubbing parameters, both for the evaluation of new materials, and for future applications of AFLCs.

2. Experimental

2.1. *Test cells*

All test cells were produced in the MC2 clean room facilities at Chalmers University of Technology.[†] The LC device fabrication technology available allows us to produce large numbers of virtually identical test cells. During the processing special attention was paid to reproducibility. Cell parameters not subject to the investigation were kept constant. All test cells have a gap of $1.2\,\mu m \pm 80\,nm$ and a pixel area of $16\,mm^2$. We studied two sets of 15 cells each, one set for each of the AFLC mixtures (W180 and W181 [6]). Within each set of 15 cells we used combinations of five different alignment layer materials and two substantially different rubbing strengths. The rubbing strength was controlled by the number of times the surface was rubbed. Five cells of each set of 15 cells were single-side rubbed, i.e. assembled from one rubbed and one non-rubbed substrate. The other ten cells had both surfaces rubbed (double-side rubbed) and were assembled in an antiparallel configuration, i.e. with the two plates having opposite rubbing directions. The rubbing direction was always chosen to be along the direction of a pixel edge. The table identifies the polyimides used as alignment layers.

The two antiferroelectric liquid crystal materials were provided by Prof. Dąbrowski (Warsaw University of Technology) and have the phase sequence I–SmA*–SmC*–SmC*$_a$. All 15 cells of each set were filled by means of capillary forces at the same time under identical conditions, using a large hot plate. The filling temperature was about 145°, i.e. about 20°C above the clearing point. After the filling was complete the cells were cooled simultaneously from the isotropic phase to the SmC$_a$* phase, assuring identical conditions of cell preparation of all cells within each set.

Table. Polyimides used for the alignment layers.

Code	Alignment layer	Supplier
PI	PI-2610	HDM
RN	RN-1286	Nissan Chemicals
AL	AL-1254	JSR
SE	SE-7992	Nissan Chemicals
MP	MP-4	MUT Warsaw

The cell code notation used in this paper is explained with the following example: RN1s04-W180. 'RN' stands for the alignment layer type (see the table), '1' indicates the number of rubbed sides (1—one-side rubbed, 2—two-side rubbed), 's' represents the rubbing strength (s—strong, w—weak), '04' refers to a parameter containing the rubbing depth or rather the pressure of the rubbing cloth onto the substrate. This parameter was kept constant for all cells in this investigation. Finally, 'W180' refers to the LC material.

2.2. *Optical and electro-optic characterization*

The phase behaviour and different textures were studied by means of polarizing microscopy using a commercial hot stage attached to the turntable of the microscope. For estimation of relative domain sizes and coverage, image analysis software was used. The various electro-optic studies and measurements were performed with a photodetector, or video camera attached to the microscope tube. Spontaneous polarization was measured by integrating the area of the current peak resulting from full switching between the two ferroelectric states when the cell was subjected to a triangular a.c. electric field. The voltages were supplied using a waveform generator and an amplifier, via electrical wires soldered onto the test cells.

3. Results and discussion

3.1. *Anticlinic vs synclinic domains*

The anticlinic structure of the SmC*$_a$ [7] phase is incompatible with any surface condition given by buffed surfaces [8], as they normally promote synclinic order. Moreover, the tendency for synclinic order is further enhanced in the case of strong polar anchoring, i.e. when the surface energies for $\mathbf{P}_s$ pointing into and out of the alignment layer are very different. Therefore, synclinic SmC* domains can persist due to surface

[†] Department of Microtechnology and Nanoscience, Chalmers University of Technology, S-412 96 Göteborg, Sweden.

action far below the bulk transition temperature to SmC^*_a [9]. Such unwanted synclinic domains cause light leakage in the zero-field state and slow down the response of AFLC cells and should therefore be suppressed.

We obtain an indication of how strong the polar/synclinic anchoring is for different combinations of AFLC materials and alignment layers by studying the ability of different alignment layers to sustain synclinic domains at zero field before and after switching; see figure 2, which shows photomicrographs of the cell AL1s04-W181. The anticlinic domains are dark when viewed between crossed polarizers oriented along and perpendicular to the smectic layers, whereas the synclinic domains appear bright. Using image analysis software, we estimated the relative area of anticlinic and synclinic domains in three stages of the investigation: (a) the virgin state obtained after cooling from the isotropic down to bulk SmC^*_a temperatures, (b) after application of a voltage ($V \ll V_{th}$, where V_{th} corresponds to the voltage for switching from the antiferroelectric to ferroelectric state), and (c) after prolonged switching with a.c. voltage at amplitudes larger than V_{th}. The measured relative area occupied by anticlinic domains was then compared for the different test cells.

3.1.1. Virgin state. We call the state obtained by cooling the liquid crystal sample from the isotropic phase to room temperature, and before any electric field treatment, the *virgin state*. An example of a typical virgin state texture is presented in figure 2 (*a*). The anticlinic domains are dark and we see that a major part of the cell area consists of bright synclinic ferroelectric 'up' and 'down' domains, implying that the LC material is essentially still in the SmC* state.

We measured the relative area of the as-formed anticlinic domains in the virgin state for the different test cells. The measurements were performed 48 h after cooling the sample to the SmC^*_a phase; results are summarized in figure 3. In general, the virgin state, after 48 h at room temperature, still consists of less than 10% anticlinic domains. This indicates that the interaction with the surfaces promotes a synclinic SmC* state, which is then elastically transferred to the bulk. In even thinner cells this effect can even make the SmC* phase stable. Thus, the interfaces play a major role in thin cells, and can easily shift the bulk transition temperature. We find that the transition from the SmC* to the SmC^*_a state in the two AFLC materials studied is strongly suppressed in thin cells, and the transition could be shifted down by several tenths of a degree. The apparent synclinic anchoring strength also depends on the alignment material and its rubbing treatment. Moreover, the relative area of anticlinic domains is larger in single side rubbed cells than in double-side rubbed cells; this could be for several reasons. First, in these cells there is no conflict in alignment from the two surfaces, cf. the surface electroclinic effect. Second, the

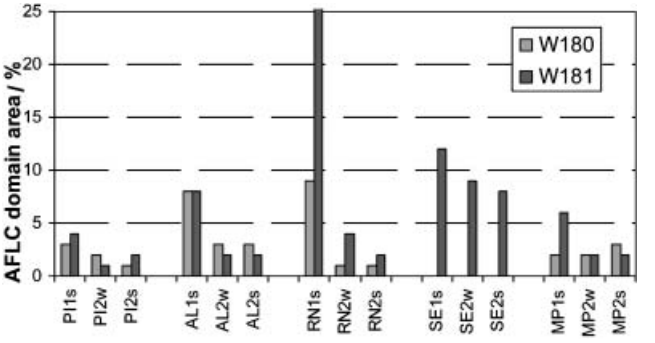

Figure 3. Measured virgin AFLC domain area with respect to the total pixel area, see figure 2. (SE cells with W180 did not develop any virgin AFLC domain).

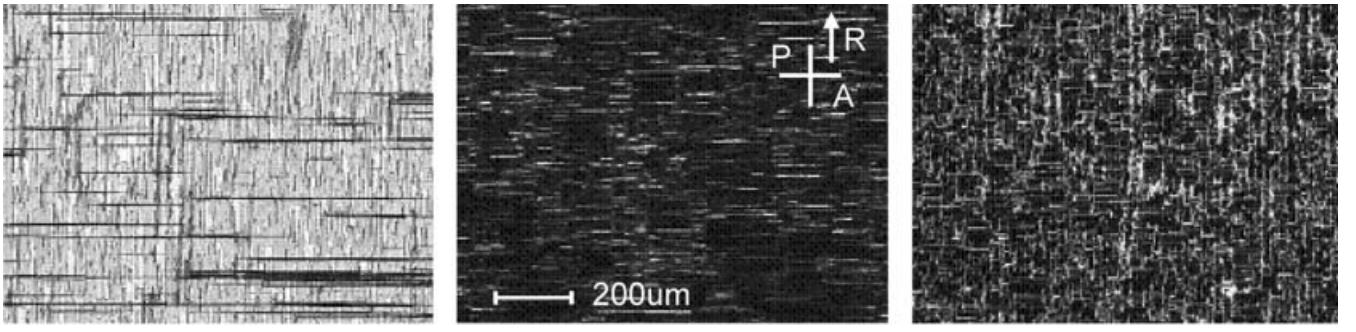

(*a*) (*b*) (*c*)

Figure 2. Texture of a cell (AL1s04-W181, room temperature) in three stages of cell investigation: (*a*) virgin state (*b*) after application of a voltage ($V \ll V_{th}$), and (*c*) after prolonged switching. The photos show that a small sub-threshold voltage seems to stimulate the relaxation from synclinic to anticlinic states in a virgin cell. When the cell is fully switched, a striped texture appears, possibly a result of the formation of horizontal chevrons after the straightening of the virgin vertical chevrons.

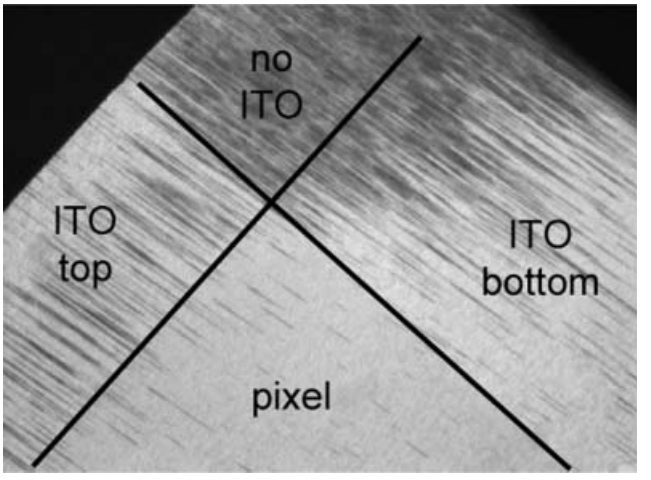

Figure 4. Virgin AFLC state in various cell areas (black stripes represent AFLC domains), cell RN1s04-W180.

rubbed surface favours one sign of ferroelectric domain (up or down); there are thus fewer domain walls in the sample and faster AFLC domain expansion during a virgin state formation (see § 3.2). Third, the asymmetric surface conditions in single side rubbed cells could favour a tilted layer structure rather than a chevron structure, which would limit the number of zig-zags. Some possible effects of a horizontal chevron surface will be discussed later.

A general feature in all the cells studied is that the presence of an ITO electrode layer between the alignment layer and the glass substrate seems to promote synclinic order, see figure 4. The photomicrograph shows a corner of the pixel. The pixel electrode (pixel) is formed by the overlap between the top electrode and the bottom electrode. Thus, four areas with different ITO/alignment layer combinations are visible. The area with the highest coverage of anticlinic domains is the 'no ITO' area located outside the pixel. In the 'pixel' there are almost no anticlinic domains, indicating an unfavourable influence of ITO on the formation of the anticlinic state. This is a general feature for all the cells studied. The ITO layer could have an effect on the strength of polar anchoring, i.e. in the ITO areas the synclinic states are favoured. However, we can see no difference in the angle of surface electroclinic effect inside and outside the ITO layers, which perhaps speaks against the polar anchoring hypothesis. The influence from the ITO layers could in fact be that the effective cell gap is smaller in these areas. Other studies have shown a clear difference in synclinic vs anticlinic domain coverage between cells with differences in cell thicknesses less than 0.1 μm [10]. The smectic layers (following the direction of black stripes) are not parallel to the pixel edge (i.e. not perpendicular to the rubbing direction) because of the SEC effect explained in § 3.2.

3.1.2. Application of a low voltage: 'stimulated relaxation' to the anticlinic state. The Application of a small a.c. electric field has a dramatic effect on the ratio of anticlinic domains: they grow in expense of the synclinic domains. The effect is already visible at $V=1.5$ V for a 50 Hz square wave, which is far below the threshold for the field-induced synclinic state ($V_{th}\approx 12.5$ V). The growing anticlinic domains are constrained in one direction along the smectic layers, while in the perpendicular direction they are pinned by zig-zag defects, and to some extent by previously developed walls between SmC* up and down domains, see figures 5 (*a*) and 5 (*b*). A small electric field allows the anticlinic domain to grow up to the closest zig-zag or domain wall, which again slows down the domain growth. After 'passing through' the zig-zag wall, the speed of domain growth increases again. This step-wise process is the subject of further studies, see

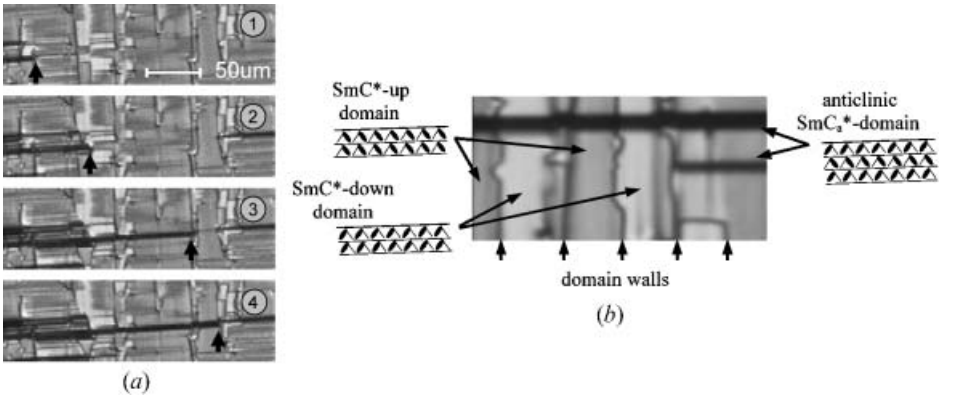

Figure 5. (*a*) A sequence of step-wise anticlinic domain expansion along the layers induced by a sub-threshold electric field; (*b*) an anticlinic domain surrounded by zig-zag domains and synclinic up and down domains and related domain walls (AL2s04-W180).

figure 5 (*a*). The effect of the electric field seems, however, to be a lowering of the energy barrier between the metastable synclinic state induced by the surfaces and the thermodynamically stable anticlinic state. This could be related to a field-induced straightening, or flexing, of the vertical chevron, making the layer structure more compatible with the essential vertical smectic layers inside the zig-zag defect.

Figure 6 (*a*) summarizes the results of this 'stimulated relaxation' from the synclinic to the anticlinic state. A comparison with the results of figure 3 shows that the application of a sub-threshold electric field significantly increases the number of anticlinic domains within the pixel, as can be seen in figure 2 (*b*). In the majority of the samples, we could obtain the anticlinic state in more than 80% of the total pixel area by the application of sub-threshold fields. For cells with a given alignment layer the results do not vary by more than 10%, even though there is a noticeable difference in alignment quality. Generally we get 'higher quality' alignment in one-side rubbed cells than in their two-side rubbed equivalents, as discussed earlier.

3.1.3. After prolonged switching: striped texture. The application of a.c. fields with an amplitude higher than the switching threshold for a prolonged time (continuous switching) usually leads to a degradation of the alignment quality. This is of course a serious drawback of present AFLC devices. Straightening of the initial vertical chevron layer structures is a well known effect that results in horizontal layer buckling [11] (often referred to as horizontal chevrons). Such a striped or quasi-bookshelf texture is visible as a grid of bright and dark lines, see figure 2 (*c*). Figure 6 (*b*) summarizes the measured area of anticlinic domains with respect to the total pixel area, after long continuous switching. Rather unexpectedly, the relative area of anticlinic domains is almost the same in figures 6 (*a*) and 6 (*b*). This suggests that the remaining synclinic domains, after straightening the vertical chevrons, are mainly due to the influence by surface action. We know that the shrinking of the equilibrium smectic layer thickness at the phase transition between the orthogonal SmA* phase and the tilted SmC* (or SmC_a*) phase, together with the condition that the layers do not slip on the surfaces, gives rise to the well known vertical chevron profiles [3]. This surface, approximately situated in the middle between the two substrates, is by symmetry non-polar and promotes planar anchoring, i.e. it could sustain both anticlinic and synclinic domains. Hence, in the virgin state we could also expect an aligning effect of the horizontal chevron surface. The energy barrier for the transition from a synclinic to an anticlinic horizontal chevron surface might be significant for the very slow relaxation from synclinic to anticlinic order in the virgin state.

3.2. *Surface electroclinic effect*

Ideally, for easy manufacturing, the layer normal in the smectic phase should be everywhere parallel to the rubbing direction. Then, by simply rubbing the two polyimide surfaces in parallel we should easily achieve a homogeneous bookshelf structure at the isotropic to smectic A phase transition. In the absence of a nematic phase between the isotropic and the SmA* phases, however, the smectic layers do not form perpendicular to the rubbing direction, but at a finite angle α. Detailed studies have revealed that the molecules remain anchored at the surface along the rubbing direction while the bulk optic axis (parallel to the smectic layer normal) is rotated with respect to the rubbing direction [12, 13]. This effect has been attributed to a polar interaction between the LC molecules and the interface, and is commonly known as the surface electroclinic effect (SEC effect) [2, 14].

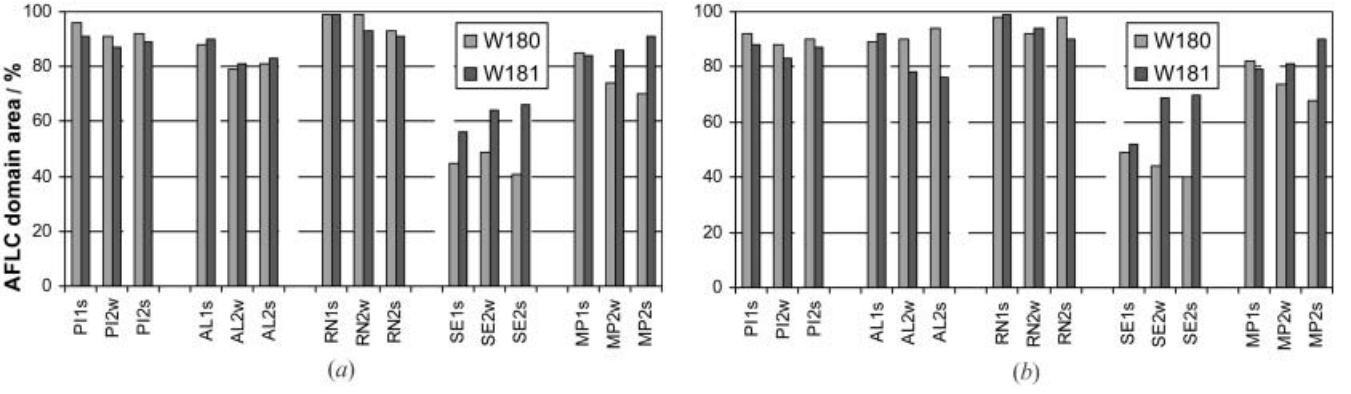

Figure 6. Measured area of anticlinic domains with respect to the total pixel area (*a*) after low voltage application, (*b*) after prolonged switching.

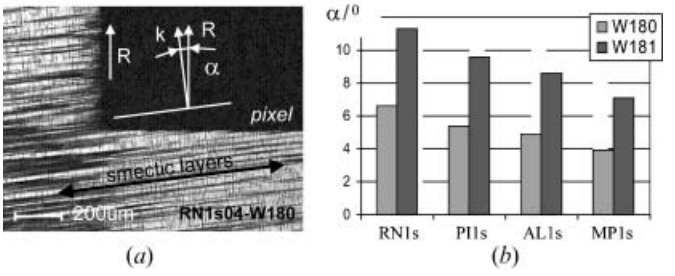

Figure 7. Surface electroclinic effect: (*a*) apparent deviation of layer normal **k** away from rubbing direction R; (*b*) clear tendency of α decreasing with decreasing $\mathbf{P}_s$ regardless of the LC material.

The angle α induced by the SEC effect depends on, at least, the two following parameters: (1) the spontaneous polarization of the LC material, i.e. materials with comparatively higher polarization exhibit a larger value of α; and (2) the rubbing strength, i.e. the SEC effect generally decreases for higher rubbing strengths. The surface electroclinic effect must be ruled out by proper choice of alignment layers, types of buffing and the liquid crystal material itself. We have studied the apparent α of the surface electroclinic effect for a certain LC material as a function of different polyimides using constant rubbing strength. We measured α in one-side rubbed cells, in which the unrubbed surface does not induce a conflict in the obtained layer orientation as would be the case in double-side rubbed cells.

Figure 7 (*a*) illustrates the consequence of the SEC effect. The smectic layer normal **k** does not coincide with the rubbing direction R, but deviates by the angle α. Our results show that different polyimides, all treated with the same rubbing strengths, give rise to different values of α for the same LC material. This indicates not only that the polar properties of the liquid crystal and the rubbing strength play a role, but also that the alignment material itself has a substantial influence on the magnitude of the SEC effect. The angles α are measured in the virgin state, i.e. the effect on the apparent α from any layer tilt is not considered. We know, however, that for nematics the pretilt angle at the surface generally depends on the buffing strength, and it is likely that we could also have a similar effect for smectics, i.e. there could in fact be a (small) pretilt-induced layer tilt in the SmA phase. We have, however, not considered such tilted layers here. Figure 7 (*b*) shows the behaviour of α for the different polyimides. The angle α is always highest in RN-type cells and lowest in MP-type cells, regardless of the LC material. There also seems to be a correlation between α and $\mathbf{P}_s$ (W181: $\mathbf{P}_s \approx 180\,\mathrm{nC\,cm^{-2}}$, W180: $\mathbf{P}_s \approx 130\,\mathrm{nC\,cm^{-2}}$). It should be noted, however, that there is also an (at least allowed) contribution from the chiral geometrical molecular structure to the surface electroclinic effect.

3.3. *Electro-optic response*

Figure 8 (*a*) shows a typical transmission–voltage characteristic of a sample driven with an increasing and decreasing square wave voltage (sqw) of 50 Hz. Each point of this characteristic is an averaged optical response for a sqw with specific amplitude; this makes the response fully symmetric around the 0 V axis. Although the shape of the characteristic looks quite similar to that obtained by driving the sample with a triangular (tri) wave at low frequency, we wish to point out that it is qualitatively and quantitatively different. (At 50 Hz the molecules are likely to switch directly between the ferroelectric states without relaxing to the anticlinic state when passing through $E=0$. At 1 Hz the sample generally has time to relax back to the anticlinic state close to $E=0$. This will be discussed in the next paragraph.) Moreover, the threshold value for the sqw is not influenced by the charge-induced ionic motion, and therefore is usually lower (at least at $f < 100$ Hz)

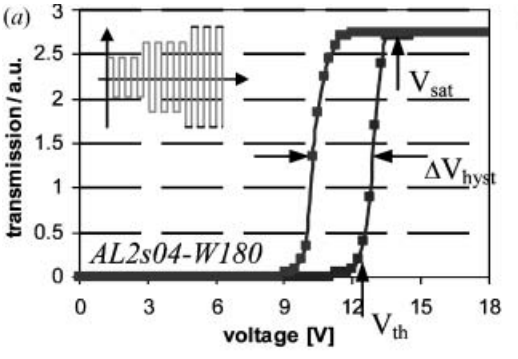

(*b*)

	W180	W168	W181	
PI cells	10.42	4.25	9.40	[V]
AL cells	12.58	5.13	10.33	[V] ← the strongest
RN cells	10.42	4.33	9.80	[V]
SE cells	10.87	n.m.	9.27	[V]
MP cells	11.25	4.33	9.10	[V]

Figure 8. (*a*) Typical TV characteristic of the cell driven with increasing/decreasing sqw wave. (*b*) averaged threshold voltages measured in the cells with various polyimide layers; vertical chevrons have been straightened.

than that found with the low frequency tri wave. (At higher frequencies, $f \sim 1000$ Hz, the threshold voltage increases with increasing frequency, mainly due to viscosity effects.) The shape of the hysteresis (the slope and the width) is also different. One can describe the characteristic by three basic parameters: V_{th}—threshold voltage (voltage when the overall transmission reaches 10%), V_{sat}—saturation voltage (voltage when the transmission reaches 100%) and ΔV_{hyst}—hysteresis (ΔV at 50% transmission). We have found that these parameters vary significantly for different alignment conditions.

The data block in figure 8 (*b*) presents the averaged threshold voltages in cells with various polyimide alignment layers. Generally, the threshold voltages are very different even for the same LC material. In our experiments, the highest threshold voltage was always found in the AL-type cells, independent of the liquid crystal. These variations could be related to the voltage drop over the alignment layer (plus surface anchoring properties). The polyimide layers differ in dielectric constant and vary slightly in thickness. These factors modify the applied field and determine the real voltage applied over the LC layer. Usually, higher threshold fields are detected in one-side rubbed cells compared with double-side rubbed cells. On the other hand the hysteresis loop was found to be wider in double-side rubbed cells. This implies that lower threshold fields and better stability of tri-state switching is found in double-side rubbed cells. We also know that the switching dynamics of AFLC materials depend on the degree of surface stabilization i.e. the degree to which the bulk helix is suppressed by means of surface forces), and also whether the tilt plane is parallel to the cell surfaces or not [15]. We have not considered the degree of surface stabilization in the cells studied. However, the pitch of these materials is in the submicron range ($\sim 0.5\,\mu$m), and in 1.5 μm thick cells, only metastable surface-stabilized states are likely. We can therefore consider the helical state the ground state in these cells.

3.4. *Relaxation to the anticlinic state during bipolar switching*

The ideal tri-state switching characteristic obtained by driving the sample with a tri wave at low frequency features a double hysteresis loop with three clearly separated optical states: ferro-up (synclinic), ferro-down (synclinic) and antiferro (anticlinic) state. Since ferro-up and ferro-down states are optically identical (they appear as equally bright states for the same voltage amplitude with different polarity) they will be called the *F-state*. The antiferroelectric state appears as a dark state when the tri wave passes 0 V and will be called the AF-state. In regime conditions, in the middle of the continuous switching process, the AF-state appears when passing 0 V, only when there is enough time for the molecules to relax from a synclinic to the anticlinic state, see also [16]. The relaxation process is driven by the antiferroelectric interaction, and is modified by the surface anchoring properties. The full AF relaxation, usually observed at very low frequencies, appears in the middle of the transition between two F-states, resulting in a pure double hysteresis loop as the characteristic optical response, see figure 9 (*a*). For high frequencies there is insufficient time for the relaxation process to complete because the applied voltage drives the molecules continuously between two F-states. At intermediate frequencies one usually observes a partial relaxation process, which manifests itself in two transition types present at the same time: F–F transition as in the case of high freqency driving, and F–AF–F transition as in the case of low frequency driving. The area of the relaxed domains strongly depends on the frequency (the lower the frequency the more domains relax to the AFLC-state) and results in a change of optical transmission. The partially relaxed cell again requires a threshold voltage (in fact it is only required for the relaxed AFLC domains) to switch to one of the F-states.

Figure 9 (*b*) shows a series of microscopic textures observed during switching between two F-states separated by a partial relaxation process. The pictures are taken at specific times with respect to the driving frequency (tri wave at $f = 0.5596$ Hz) and correspond to the points marked on the TV characteristic, see figure 9 (*a*). The white colour in the first picture represents the bright state formed by switched F-domains; small dark spots represent AF-domains which are in the anticlinic state. Decreasing the field collectively rotates the F-domains, resulting in a decrease of transmission level (grey scale in pictures 2 to 4). In picture 5, a rapid expansion of AF-domains is observed, which remain anticlinic up to picture 8, whereas the remaining F-domains continuously rotate to the opposite F-state (pictures 5 to 7). Picture 7 clearly shows the consequence of the partial relaxation as the coexistence of two separated domains (F- and AF-domains). The relaxed AF-domains undergo a transition to the F-state only when the threshold is reached, i.e. a few ms after picture 8 was taken. That transition is visible as a shrinkage of AF-domains (picture 9) and an increase of the optical transmission. Finally, in picture 10 a fully switched F-state is obtained.

Figure 9 (*c*) shows the TV characteristic of the same cell but under transient condition where the driving starts from a fully relaxed state (only AF-domains). The

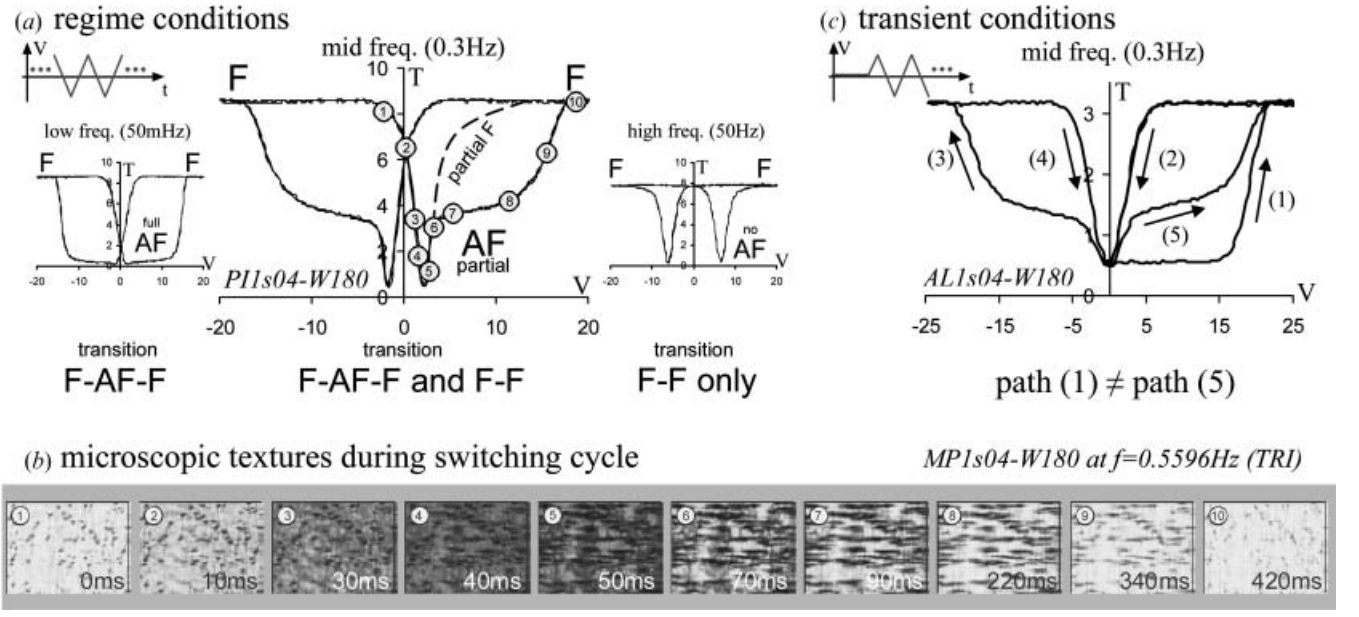

Figure 9. (*a*) Typical TV characteristics of AFLC cells at various frequencies at regime conditions; (*b*) textures during a switching cycle; (*c*) TV characteristic of an AFLC cell under transient conditions.

transient path (1) significantly differs from the regime path (5), which confirms that during repeated switching the sample only partially relaxes to the original state. Note that both threshold voltage and saturation voltage remain constant, i.e. they are independent of the amount of AF-domains in the sample.

We found that the partial relaxation process does not depend only on the driving conditions (voltage or frequency) but is also influenced by the alignment layer and its treatment. The amount of relaxed AF-domains differs for different surfaces even with identical driving conditions. Figure 10 (*a*) presents the TV characteristics of three samples with the same alignment layer (RN type) and different rubbing parameters. The measurements were performed with the same driving voltage and the same frequency. Three different levels of relaxation are clearly visible. In the one-side rubbed cell about 96% of anticlinic domains have developed, while in the two side-rubbed cells (2w, 2s) only 42% and 68% respectively. We have estimated the speed of the relaxation process by tuning the driving frequency to obtain 50% anticlinic and 50% synclinic domains. The results are shown in figure 10 (*b*), by plotting the necessary frequency for 50% relaxation in various cells. In general, the fastest relaxation (the highest frequency on the graph) was found in one-side rubbed cells (1s type). Although the frequencies are quite similar for both types of two-side rubbed cells (with the same alignment layer), there is a tendency for faster relaxation in strongly rubbed cells (2s type) when compared with the more weakly rubbed ones (2w type). From the above measurements one may conclude that one-side rubbing as well as stronger double-side rubbing are preferred for faster relaxation.

Finally we would like to comment on the shape of the TV characteristic with partial relaxation process, which in some cells—middle graph in figure 10 (*a*)—strongly resembles the so-called V-shaped switching

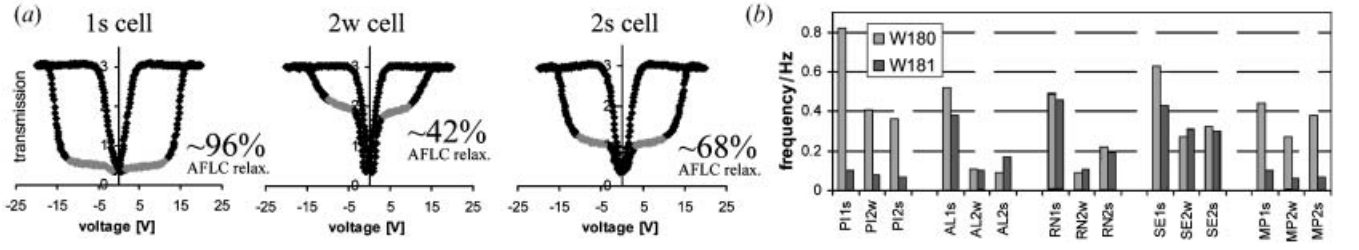

Figure 10. Optical response of a partial relaxation to the AFLC state in cells with various rubbing conditions (RN*xx*04-W180). (*b*) Frequency values of the driving voltage obtained for a 50% AFLC relaxation.

characteristic. However, the AFLC state, to which the cell relaxes, cannot give rise to thresholdless/V-shaped switching [17–19]. The fact that the slopes overlap is caused by the interaction of surfaces with the continuous director reorientation between two F-states, giving the illusion of a V-shaped-like characteristic.

4. Conclusions

In this paper, we have reported on the strong influence of different alignment materials on the switching behaviour and alignment properties of antiferroelectric liquid crystals in bookshelf device cells. We have shown that in thin cells, i.e. useful cells for applications with the two AFLC materials studied, the surface influence can totally dominate the dynamics of the cells. On cooling in the absence of electric fields, from the isotropic, through SmA*, SmC*, and SmC_a* phases, only a few percent of antiferroelectric domains develop in the cells studied. The remaining area stays in the SmC* state (ferroelectric domains). Clearly the surface effects suppress the transition to the SmC^*_a state. The synclinic states are metastable and relax very slowly to the anticlinic state. (In even thinner cells, we may talk about surface-stabilized phase behaviour, as the SmC^*_a phase can be totally suppressed in favour of the synclinic SmC* phase, making the synclinic state correspond to a global energy minimum.) The application of a field, much lower than the AF–F threshold, promotes or 'stimulates' the relaxation from ferroelectric to antiferroelectric domains. We have also shown that the unwanted surface electroclinic effect is also dependent on the choices of AFLC material and type of rubbed surface alignment layers.

Our results indicate that it is not enough to evaluate different AFLC materials in only one type of cell. Neither is it enough to evaluate surface alignment layers using only one AFLC material. Instead we must always evaluate and optimize the AFLC materials and the surface alignment methods in parallel. We show that the combination of surface alignment layers and liquid crystal materials is crucial for the development of AFLC devices. In our case, double-side buffed samples exhibit lower threshold voltages and better tri-state stability, but the alignment quality is higher and the relaxation from F to AF is faster in single-side rubbed cells. The different degrees of partial AFLC relaxation observed by using different interfaces might give important information for the optimization of AFLC materials, surface layers, and driving waveforms.

Acknowledgements

This work is supported by the Belgian IAP5/18, BWS project Flanders/Poland, EU project SAMPA, the Swedish Research Council, and the Swedish Foundation for Strategic Research.

References

[1] J. Cognard. *Mol. Cyst. liq. Cyst.*, **51**, 1 (1982).
[2] J. Xue, N.A. Clark. *Phys. Rev. Lett.*, **64**, 307 (1990).
[3] N.A. Clark, T.P. Rieker. *Phys. Rev. A*, **37**, 1053 (1988).
[4] A. Jakli, A. Saupe. *Phys. Rev. A*, **45**, 5674 (1992).
[5] J. Pavel, M. Glogarova. *Liq. Cryst.*, **9**, 87 (1991).
[6] R. Dąbrowski. *HEMIND* Report, January (2003).
[7] A.D.L. Chandani, E. Górecka, Y. Ouchi, H. Takezoe, A. Fukuda. *Jpn. J. appl. Phys.*, **28**, L1265 (1989).
[8] S.T. Lagerwall. *Ferroelectric and Antiferroelectric Liquid Crystals*. Wiley-VCH (1999).
[9] P. Rudquist, J.P.F. Lagerwall, M. Buivydas, F. Gouda, S.T. Lagerwall, N.A. Clark, J.E. Maclennan, R. Shao, D.A. Coleman, S. Bardon, T. Bellini, D.R. Link, G. Natale, M.A. Glaser, D.M. Walba, M.D. Wand, X.-H. Chen. *J. mater. Chem.*, **9**, 1257 (1999).
[10] P. Rudquist, K. D'Havé, S.T. Lagerwall, R. Dąbrowski. In Proceedings of the 20th International Liquid Crystal Conference, Ljubljana, Slovenia, APPL-P117 (2004).
[11] S.T. Lagerwall, K. D'Havé, P. Rudquist. *Proc. SID Dig.*, 120 (2001).
[12] K. Nakagawa, T. Shinomiya, M. Koden, K. Tsubota, T. Kuratate, Y. Ishii, F. Funada, M. Matsuura, K. Awane. *Ferroelectrics*, **85**, 39 (1998).
[13] W. Chen, Y. Ouchi, T. Moses, Y.R. Shen, K.H. Yang. *Phys. Rev. Lett.*, **68**, 1547 (1992).
[14] M.S. Spector, S.K. Prasad, B.T. Weslowski, R.D. Kamien, J.V. Selinger, B.R. Ratna, R. Shashidhar. *Phys. Rev. E*, **61**, 3977 (2000).
[15] P. Rudquist, J.G. Meier, J.P.F. Lagerwall, K. D'Havé, S.T. Lagerwall. *Phys. Rev. E*, **66**, 061708 (2002).
[16] P. Rudquist, D. Krüerke, S.T. Lagerwall, J.E. MacLennan, N.A. Clark, D.M. Walba. *Ferroelectrics*, **246**, 21 (2000).
[17] A. Adamski, H. Pauwels, K. Neyts, C. Desimpel, S. Vermael. *Proc. SPIE*, **4759**, 127 (2002).
[18] H. Pauwels, A. Adamski. *Ferroelectrics*, **277**, 125 (2002).
[19] A. Adamski, H. Pauwels, K. Neyts. *Liq. Cryst.*, **31**, 997 (2004).